Ester-Linked Crystalline Covalent Organic Frameworks

Chenfei Zhao,† Hao Lyu,† Zhe Ji,† Chenhui Zhu,‡ and Omar M. Yaghi†,*

†Department of Chemistry, University of California—Berkeley; Kavli Energy Nanoscience Institute at UC Berkeley; and Berkeley Global Science Institute, Berkeley, California 94720, United States

‡Advanced Light Source, Lawrence Berkeley National Laboratory, Berkeley, California 94720, United States

ABSTRACT: Ester-linked, crystalline, porous, covalent organic frameworks (COFs) have been synthesized and structurally characterized. Transesterification reactions between di-topic 2-pyridinyl aromatic carboxylates and tri- or tetra-topic phenols gave the corresponding ester-linked COFs. They crystallize as 2D structures in **kgm** (COF-119) and **hcb** (COF-120, 121, 122) topologies with surface areas of up to 2,092 m^2/g. Notably, crystalline COF-122 comprises edges spanning over 10 phenylene units; an aspect had only been achieved in metal–organic frameworks. This work expands the scope of reticular chemistry to include for the first time crystalline ester-linked COFs, related to common polyesters.

Ester is one of the most common functionalities in organic chemistry; however, it is yet to be reported as a linkage in covalent organic frameworks (COFs).[1,2] Despite the ubiquity of polyester materials,[3] their porous, crystalline, cross-linked counterparts are undeveloped (Figure 1). In contrast to ester molecules or polyesters, developing synthetic method for ester-linked COFs is considered more challenging as it requires the simultaneous process of carrying out the esterification reactions and framework crystallization.

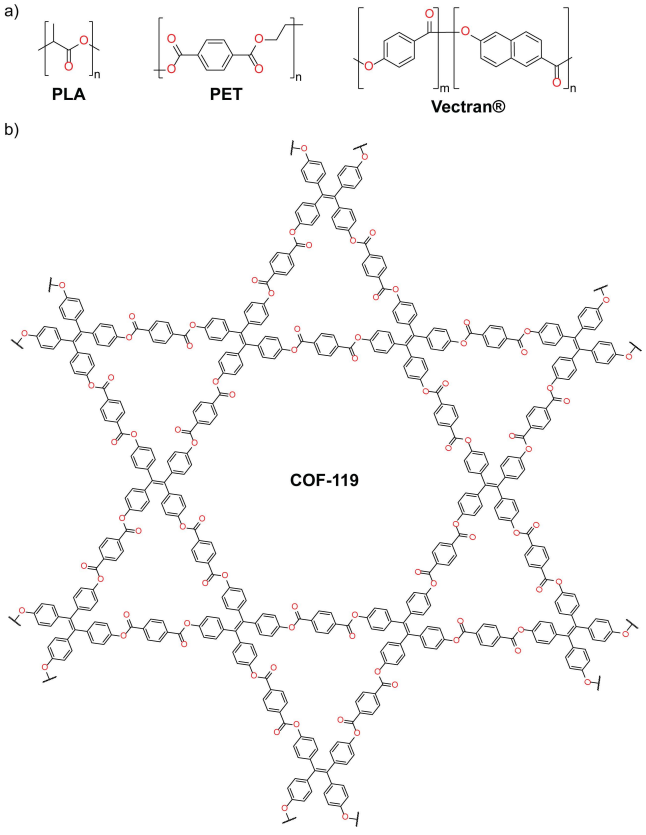

Figure 1. (a) Examples of common polyester materials: polylactic acid (PLA), polyethylene terephthalate (PET), and Vectran®. (b) Ester-linked COF targeted in this work.

New linkage development is essential to expanding the scope of reticular chemistry and it has been one of the major research directions in this area. While imine and its related linkages remain the most studied,[2] significant advances in expanding the scope of direct COF crystallization have been made in recent years. For example, linkages considered less reversible such as olefin[4] and dioxin[5] have been developed. Incorporating sp^3 carbon has also been possible in the form of the aminal linkage.[6] We expect that the 'crystallization problem' regarding the ester linkage can also be addressed by the proper combination of building units and reaction conditions. Here, we report the successful reticulation of ester-linked COFs as crystalline, porous structures.

We selected tetrakis(4-hydroxyphenyl)ethylene (THPE) along with various terephthalic acid derivatives for COF synthesis. Di(pyridin-2-yl) terephthalate (DPT) was found to be a suitable starting material in reactions leading to a

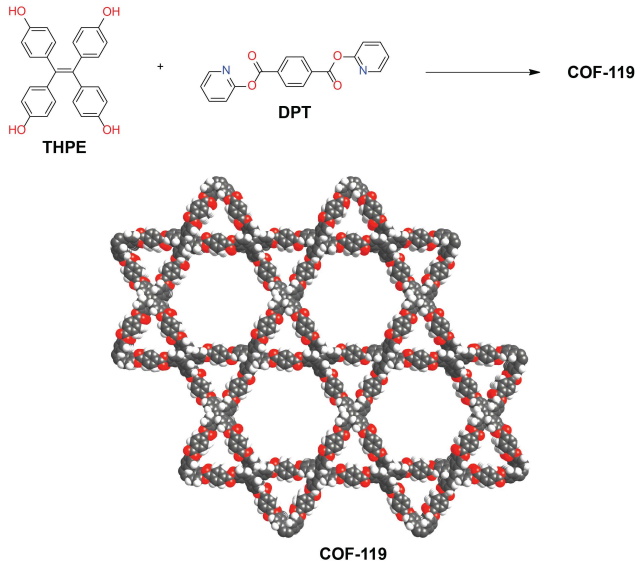

Figure 2. Synthetic scheme for COF-119. A structure model based on powder X-ray diffraction data is shown in space-filling style. Color code: H, white; C, gray; and O, red.

highly crystalline product termed COF-119, $[(THPE)(DPT)_2]_{ester}$ (Figure 2).[7] The reaction was carried out in the presence of 1,8-diazabicyclo[5.4.0]undec-7-ene (DBU) and dioxane at 150 °C in a sealed tube for 3 days. The product was insoluble in common organic solvents such as *N*,*N*-dimethylformamide, methanol, and acetone. On the other hand, no highly crystalline COF was obtained when terephthalic acid, terephthaloyl chloride, diphenyl terephthalate, or dimethyl terephthalate was used instead of DPT. This is likely because these starting materials are either too inert or too reactive to allow for a modulated crystallization process.[8] The crystallinity of COF-119 was assessed by a powder X-ray diffraction (PXRD) study (Figure 3a). Remarkably, 15 diffraction peaks were observed with a laboratory X-ray source, far more than those from the more well-developed imine-linked or boronate ester-linked COFs with otherwise identical building units.[9,10] The structure was modeled with **kgm** topology in $P\bar{3}$ space group (No. 147), and the unit cell parameters were further refined from the

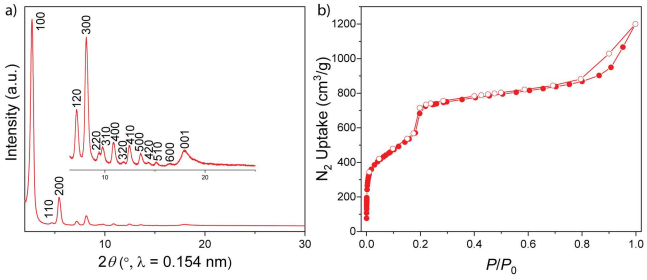

Figure 3. (a) PXRD pattern of COF-119 from a laboratory source of X-ray (Cu Kα). (b) N_2 sorption isotherm for COF-119 at 77 K.

PXRD pattern through Pawley fitting. The layers are stacked in an eclipsed mode and the unit cell parameters (a = b = 37.48 Å and c = 4.95 Å) were obtained with good agreement factors (R_p = 3.37%, R_{wp} = 4.51%). Porosity was characterized by measuring the nitrogen sorption isotherm of the activated sample at 77 K (Figure 3b). The distinct step

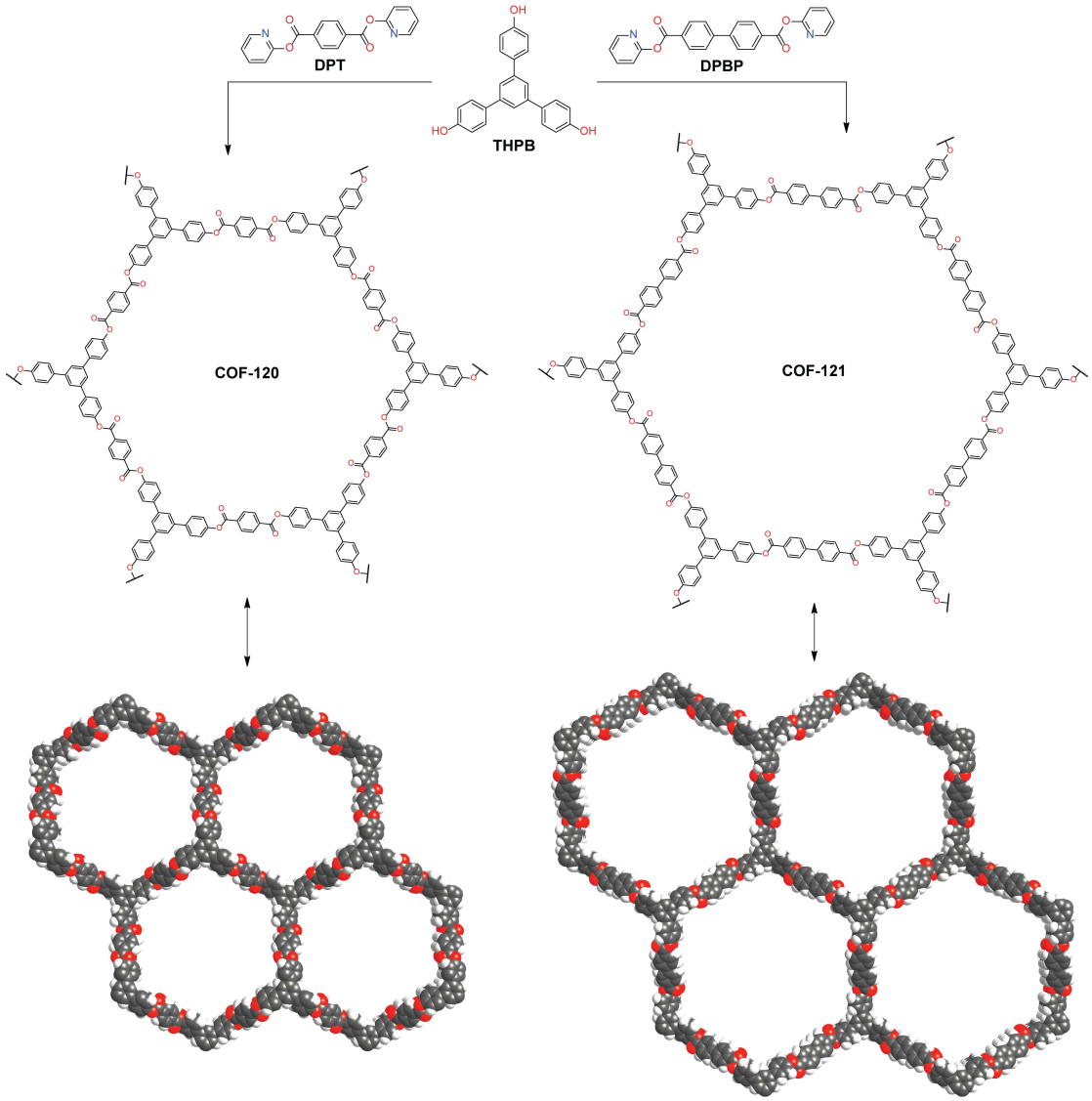

Figure 4. Synthetic scheme for COF-120 and COF-121, including their powder X-ray diffraction structure models in space-filling style. Color code: H, white; C, gray; and O, red.

between P/P_0 = 0.18–0.21 results from the mesopore filling of COF-119. The Brunauer–Emmett–Teller (BET) surface area was calculated to be 2,092 m^2/g. Calculation with the quenched solid density functional theory (QSDFT) based on the carbon model for cylindrical pores yielded pore sizes centered at 29.9 Å and 17.9 Å (Figure S37), comparable to those of the corresponding imine-linked COF (29 Å, 16 Å) based on the same model.[10b, 11] Conversion of the transesterification reaction was evaluated by Fourier transform infrared (FT-IR), ^{13}C cross–polarization magic angle spinning (CP-MAS) NMR spectroscopies, and elemental analysis (Supporting Information Section S3–5). Consumption of THPE was ascertained by the disappearance of the O-H stretching band in the COF (Figure S6). A blueshift of the ester C=O stretching mode from 1726 cm^{-1} to 1744 cm^{-1} was also noted as compared to DPT (Figure S3). On the other hand, a minor difference between the ester ^{13}C chemical shifts of DPT and COF-119 was observed (Figure S18). This is not surprising in light of the similarity between those shifts of DPT and diphenyl terephthalate, which is a close molecular analogue for COF-119. Nevertheless, the chemical shift at 158 ppm of DPT, corresponding to the C2 carbon of the pyridinyl group, is significantly attenuated in the COF. Finally, based on the residual nitrogen content, we estimate there is 1 unreacted 2-pyridinyl unit per 33 ester groups on COF-119 (see Section S5).[12]

The synthetic method for COF-119 was also applied to new COFs with **hcb** topology. Specifically, reticulation of 1,3,5-tris(4-hydroxyphenyl)benzene (THPB) with DPT gives COF-120, $[(THPB)_2(DPT)_3]_{ester}$, or with di(pyridin-2-yl) [1,1'-biphenyl]-4,4'-dicarboxylate (DPBP) gives COF-121, $[(THPB)_2(DPBP)_3]_{ester}$ (Figure 4). The crystallinity of these materials is lower compared to that of COF-119, as evidenced by the observation of fewer diffraction peaks in their PXRD patterns (Figure 5a, b). The superior crystallinity of COF-119 is likely a result of better interlayer stacking endowed by the tetraphenylethylene units.[10b]

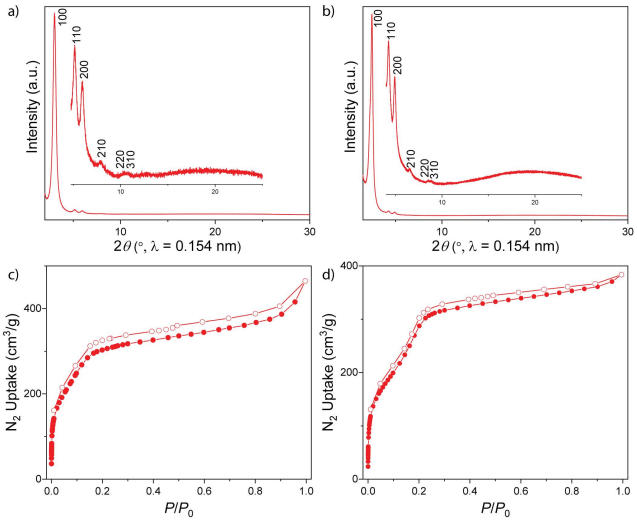

Figure 5. PXRD patterns of (a) COF-120 and (b) COF-121, measured with a laboratory source of X-ray (Cu Kα), and N_2 sorption isotherms of (c) COF-120 and (d) COF-121 at 77 K.

The structures were modeled in space group $P\bar{3}$ (No. 147) with Pawley fitting performed against their PXRD patterns. The unit cell parameters (COF-120: $a = b$ = 34.29 Å and c = 4.17 Å; COF-121: $a = b$ = 41.27 Å and c = 4.28 Å) were obtained with good agreement factors (COF-120: R_p = 3.61%, R_{wp} = 4.95%; COF-121: R_p = 6.43%, R_{wp} = 7.88%). Although the models are based on eclipsed stacking between the COF layers, the presence of other stacking modes cannot be ruled out due to inadequate diffraction data as a result of the low crystallinity of these materials. The porosity was characterized by nitrogen sorption isotherms measured on the activated samples at 77 K, which gave BET surface areas of 1,255 m^2/g and 908 m^2/g for COF-120 and COF-121, respectively (Figure 5c, d). The lack of highly distinctive steps of mesopore filling from these isotherms is attributed to stacking disorders of COF-120 and COF 121. FT-IR and ^{13}C CP-MAS NMR results of these materials are within expectation and free of noticeable impurities (Section S3, S4). The conversions of the transesterification reactions on the COFs were estimated from residual nitrogen contents to be 95% and 90% for COF-120 and COF-121, respectively (Section S5).

The structural models were built and geometrically optimized using the Forcite module in Materials Studio (Section S10). Regarding COF-120 and COF-121, the unit cell parameters a and b of fully relaxed models are notably larger than those determined by the experimental X-ray diffraction patterns (Table 1, Entry 1, 2). On the other hand, such discrepancy is less pronounced for COF-119. Smaller experimental a and b values are likely due to favorable framework contractions to decrease void spaces within the COFs, which are facilitated by flexible ester linkages.[13] As a result, COF-120 and COF-121 are likely to adopt more corrugated hexagonal conformations (Section S7). The smaller trigonal pores of COF-119 serve as an additional hurdle for framework deformation. The ordered stacking between the tetraphenylethylene units may also contribute to the structural rigidity of COF-119.[10b] To further elucidate the rigidity difference between these materials, we compared the X-ray diffraction positions of both dry and solvated COFs (Figure S23). In contrast to COF-119, more evident shifts of the diffraction positions towards lower angle were observed for COF-120 and COF-121, indicating framework expansion of these materials in their solvated forms (Table 1, Entry 2, 3).[14]

Table 1. Unit cell parameters $a = b$ (Å) for ester-linked COFs.

Entry	Source	COF-119	COF-120	COF-121
1	Relaxed Model	37.70	37.02	44.16
2	WAXS[a]	37.55	34.36	41.34
3	WAXS (CH_3CN)[a]	37.16	35.99	43.02

[a] Wide-angle X-ray scattering (WAXS). Samples were measured in capillary tubes with synchrotron X-ray. Unit cell parameters $a = b$ here were directly calculated from the (100) diffraction positions.

To further explore the scope of the method, extended di- and tri-topic building units were used to construct a hexagonal COF with the largest pore size to date (Section S2).[2d,15,16] Insoluble crystalline product was isolated with an ester conversion of 97% (Section S5). Based on the corresponding WAXS data, a distorted hexagonal structure was modeled, with each edge spanning 10 phenylene units and

2 ester linkages (Figure 6a, b). Nevertheless, stacking mode between the layers is not assigned due to the low crystallinity and porosity (BET surface area: 646 m^2/g, Figure S35, 36). Similar to the other ester-linked COFs with **hcb** topology, COF-122 undergoes unit cell expansion when solvated in acetonitrile, as evidenced by the shift of diffraction positions towards the lower angle (Figure 6c). Further studies are underway to firmly establish the detailed structure of COF-122. These efforts are currently challenged by the flexibility of its structure. However, it is quite remarkable that this COF based on ester linkages can be crystallized with edges containing ten phenylene units; an aspect only achieved in the chemistry of metal-organic frameworks and pointing to the level of progress being achieved in COF chemistry.[2e, 17]

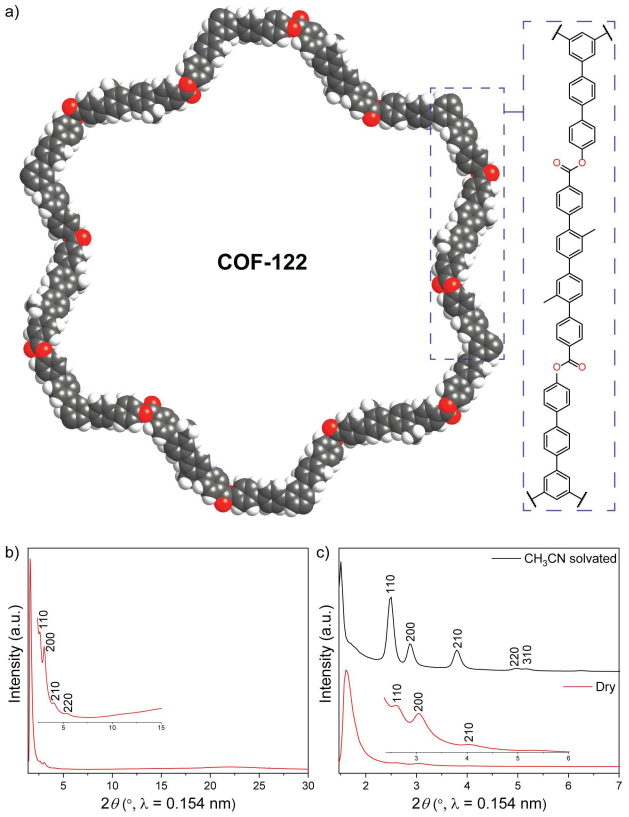

Figure 6. (a) Space filling diagram of one hexagon unit of activated COF-122. Color code: H, white; C, gray; and O, red. (b) WAXS pattern of activated COF-122. (c) Comparison between WAXS patterns of activated and CH_3CN-solvated COF-122.

In summary, we developed the first synthetic method to access crystalline, porous COFs with ester linkages. Transesterification reactions between di-topic 2-pyridinyl aromatic carboxylates and tri- or tetra-topic phenols provided COFs with **kgm** and **hcb** topologies. The difference in topology also resulted in markedly different crystallinity and framework rigidity. This method also led to crystallization of a hexagonal COF with the largest edge length.

ASSOCIATED CONTENT

The supporting information is available free of charge via the Internet at http://pubs.acs.org.

Methods and additional data (PDF)

AUTHOR INFORMATION

Corresponding Author

Omar M. Yaghi – Department of Chemistry, University of California—Berkeley; Kavli Energy Nanoscience Institute at UC Berkeley; and Berkeley Global Science Institute, Berkeley, California 94720, United States, orcid.org/0000-0002-5611-3325; Email: yaghi@berkeley.edu

Authors

Chenfei Zhao – Department of Chemistry, University of California—Berkeley; Kavli Energy Nanoscience Institute at UC Berkeley; and Berkeley Global Science Institute, Berkeley, California 94720, United States; orcid.org/0000-0003-3960-3047

Hao Lyu – Department of Chemistry, University of California—Berkeley; Kavli Energy Nanoscience Institute at UC Berkeley; and Berkeley Global Science Institute, Berkeley, California 94720, United States; orcid.org/0000-0001-7393-2456

Zhe Ji – Department of Chemistry, University of California—Berkeley; Kavli Energy Nanoscience Institute at UC Berkeley; and Berkeley Global Science Institute, Berkeley, California 94720, United States; orcid.org/0000-0002-8532-333X

Chenhui Zhu – Advanced Light Source, Lawrence Berkeley National Laboratory, Berkeley, California 94720, United States

Notes

The authors declare no competing financial interest.

ACKNOWLEDGMENT

We acknowledge King Abdulaziz City for Science and Technology (KACST), Riyadh, Saudi Arabia, as part of a joint KACST–UC Berkeley Center of Excellence. We thank the College of Chemistry's NMR (CoC-NMR) facility of University of California-Berkeley for resources provided and assistance. Instruments in CoC-NMR are supported in part by NIH S10OD024998. This research used beamline 7.3.3 of the Advanced Light Source at the Lawrence Berkeley National Laboratory, which is a DOE Office of Science User Facility under contract no. DE-AC02-05CH11231.

REFERENCES

(1) (a) Côté, A. P.; Benin, A. I.; Ockwig, N. W.; O'Keeffe, M.; Matzger, A. J.; Yaghi, O. M. Porous, crystalline, covalent organic frameworks. *Science* **2005**, *310*, 1166–1170. (b) El-Kaderi, H. M.; Hunt, J. R.; Mendoza-Cortés, J. L.; Côté, A. P.; Taylor, R. E.; O'Keeffe, M.; Yaghi, O. M. Designed synthesis of 3D covalent organic frameworks. *Science* **2007**, *316*, 268–272.

(2) Selected reviews: a) Ding, S.-Y.; Wang, W. Covalent organic frameworks (COFs): from design to applications. *Chem. Soc. Rev.* **2013**, *42*, 548–568. (b) Waller, P. J.; Gándara, F.; Yaghi, O. M. Chemistry of covalent organic frameworks. *Acc. Chem. Res.* **2015**, *48*, 3053–3063. (c) Lohse, M. S.; Bein, T. Covalent organic frameworks: Structures, synthesis, and applications. *Adv. Funct. Mater.* **2018**, *28*, 1705553. (d) Chen, X.; Geng, K.; Liu, R.; Tan, K. T.; Gong, Y.; Li, Z.; Tao, S.; Jiang, Q.; Jiang, D. Covalent organic frameworks: chemical approaches to designer structures and built-in functions. *Angew. Chem. Int. Ed.* **2020**, *59*, 5050–5091. (e) Yaghi, O. M.; Kalmutzki, M. J.; Diercks, C. S. *Introduction to Reticular Chemistry: Metal-Organic Frameworks and Covalent Organic Frameworks*; Wiley-VCH: Weinheim, 2019.

(3) (a) Deopura, B. L.; Alagirusamy, R.; Joshi, M.; Gupta, B. *Polyesters and Polyamides*; Woodhead Publishing Limited: Cambridge, 2008. (b) Beers, D. E.; Ramirez, J. E. Vectran high-performance fibre. *J. Text. Inst.* **1990**, 81, 561–574.

(4) (a) Zhuang, X.; Zhao, W.; Zhang, F.; Cao, Y.; Liu, F.; Bi, S.; Feng, X. A two-dimensional conjugated polymer framework with fully

sp2-bonded carbon skeleton, *Polym. Chem.* **2016**, *7*, 4176–4181. (b) Jin, E.; Asada, M.; Xu, Q.; Dalapati, S.; Addicoat, M. A.; Brady, M. A.; Xu, H.; Nakamura, T.; Heine, T.; Chen, Q.; Jiang, D. Two-dimensional sp^2 carbon–conjugated covalent organic frameworks. *Science*, **2017**, *357*, 673–676. (c) Lyu, H.; Diercks, C. S.; Zhu, C.; Yaghi, O. M. Porous crystalline olefin-linked covalent organic frameworks. *J. Am. Chem. Soc.* **2019**, *141*, 6848–6852.

(5) (a) Zhang, B.; Wei, M.; Mao, H.; Pei, X.; Alshmimri, S. A.; Reimer, J. A.; Yaghi, O. M. Crystalline dioxin-linked covalent organic frameworks from irreversible reactions. *J. Am. Chem. Soc.* **2018**, *140*, 12715–12719. (b) Guan, X.; Li, H.; Ma, Y.; Xue, M.; Fang, Q.; Yan, Y.; Valtchev, V.; Qiu, S. Chemically stable polyarylether-based covalent organic frameworks. *Nat. Chem.* **2019**, *11*, 587–594.

(6) Jiang, S.; Gan, S.; Zhang, X.; Li, H.; Qi, Q.; Cui, F.; Lu, J.; Zhao, X. Aminal-Linked Covalent Organic Frameworks through Condensation of Secondary Amine with Aldehyde. *J. Am. Chem. Soc.* **2019**, *141*, 14981–14986.

(7) Chen, J.; Namila, E.; Bai, C.; Baiyin, M.; Agula, B.; Bao, Y.-S. Transesterification of (hetero)aryl esters with phenols by an Earth-abundant metal catalyst. *RSC Adv.* **2018**, 8, 25168–25176.

(8) The leaving group affects the reaction rate therefore its variation modulates the crystal growth process: Ma, T.; Kapustin, E. A.; Yin, X.; Liang, L.; Zhou, Z.; Niu, J.; Li, L.; Wang, Y.; Su, J.; Li, J.; Wang, X.; Wang, W. D.; Wang, W.; Sun, J.; Yaghi, O. M. Single-crystal x-ray diffraction structures of covalent organic frameworks. *Science* **2018**, *361*, 48–52.

(9) Dalapati, S.; Jin, E.; Addicoat, M.; Heine, T.; Jiang, D. Highly Emissive Covalent Organic Frameworks. *J. Am. Chem. Soc.* **2016**, *138*, 5797–5800.

(10) (a) Zhou, T.-Y.; Xu, S.-Q.; Wen, Q.; Pang, Z.-F.; Zhao, X. One-step construction of two different kinds of pores in a 2D covalent organic framework. *J. Am. Chem. Soc.* **2014**, *136*, 15885–15888; (b) Ascherl, L.; Sick, T.; Margraf, J. T.; Lapidus, S. H.; Calik, M.; Hettstedt, C.; Karaghiosoff, K.; Döblinger, M.; Clark, T.; Chapman, K. W.; Auras, F.; Bein, T. Molecular docking sites designed for the generation of highly crystalline covalent organic frameworks. *Nat. Chem.* **2016**, *8*, 310–316.

(11) Neimark, A. V.; Lin, Y.; Ravikovitch, P. I.; Thommes, M. Quenched solid density functional theory and pore size analysis of micro-mesoporous carbons. *Carbon* **2009**, *47*, 1617–1628.

(12) Trace amounts of 2-hydroxypyridine and/or DBU may be trapped in closed pores and also contribute to the nitrogen content observed in elemental analysis.

(13) In a series of postsynthetic transformations, crystallinity and surface area dropped significantly with a flexible linkage, but recovered when the linkage was subsequently rigidified: Lyle, S. J.; Osborn Popp, T. M.; Waller, P. J.; Pei, X.; Reimer, J. A.; Yaghi, O. M. Multistep solid-state organic synthesis of carbamate-linked covalent organic frameworks. *J. Am. Chem. Soc.* **2019**, *141*, 11253–11258.

(14) Solvent occupies void spaces in the frameworks therefore they are less prone to contract. Water-induced framework contraction is also known, see ref. 8 and: Chen, Y.; Shi, Z.-L.; Wei, L.; Zhou, B.; Tan, J.; Zhou, H.-L.; Zhang, Y.-B. Guest-Dependent Dynamics in a 3D Covalent Organic Framework. *J. Am. Chem. Soc.* **2019**, *141*, 3298–3303.

(15) (a) Jin, S.; Furukawa, K.; Addicoat, M.; Chen, L.; Takahashi, S.; Irle, S.; Nakamura, T.; Jiang, D. Large pore donor–acceptor covalent organic frameworks. *Chem. Sci.* **2013**, *4*, 4505–4511. (b) Fang, Q.; Zhuang, Z.; Gu, S.; Kaspar, R. B.; Zheng, J.; Wang, J.; Qiu, S.; Yan, Y. Designed synthesis of large-pore crystalline polyimide covalent organic frameworks. *Nat. Commun.* **2014**, *5*, 4503.

(16) Yu, S.-B.; Lyu, H.; Tian, J.; Wang, H.; Zhang, D.-W.; Liu, Y.; Li, Z.-T. A polycationic covalent organic framework: a robust adsorbent for anionic dye pollutants. *Polym. Chem.* **2016**, *7*, 3392–3397.

(17) Deng, H.; Grunder, S.; Cordova, K. E.; Valente, C.; Furukawa, H.; Hmadeh, M.; Gándara, F.; Whalley, A. C.; Liu, Z.; Asahina, S.; Kazumori, H.; O'Keeffe, M.; Terasaki, O.; Stoddart, J. F.; Yaghi, O. M. Large-Pore Apertures in a Series of Metal-Organic Frameworks. *Science* **2012**, *336*, 1018–1023.